Proceedings of the ASME 2010 3rd Joint US-European Fluids Engineering Summer Meeting and 8th International Conference on Nanochannels, Microchannels, and Minichannels
FEDSM-ICNMM2010
August 1-5, 2010, Montreal, Canada

FEDSM-ICNMM2010-30054

THE EFFECT OF IN-LINE OSCILLATION ON THE FORCES OF A CYLINDER VIBRATING IN A STEADY FLOW

Sofia Peppa
Department of Naval Architecture & Marine Engineering, NTUA
Athens, Greece

Lambros Kaiktsis
Department of Naval Architecture & Marine Engineering, NTUA
Athens, Greece

George Triantafyllou
Department of Naval Architecture & Marine Engineering, NTUA
Athens, Greece

ABSTRACT

In this paper we present a computational study of the forces acting on a circular cylinder vibrating both transversely and in-line to a uniform stream. The in-line vibration frequency is equal to twice the transverse frequency. The cylinder thus follows a figure-eight trajectory, emulating the trajectory of a free vortex-induced vibration. We consider three values of transverse oscillation frequency, in the regime of the natural frequency of the Kármán street, for a Reynolds number of 400.

We find that the fluid forces are greatly influenced by the direction in which the figure-eight is traversed. We also find that the spectrum of the lift force is characterized by the strong presence of odd-numbered higher harmonics. Moreover, depending on the combination of oscillation amplitude and frequency, the lift force exhibits aperiodic time dependence.

INTRODUCTION

Several engineering structures exhibit vibration problems, arising from the flow dynamics. In particular, in structures as oil risers and heat exchangers, excitation is due to the formation of the Kármán vortex street, which results in time-dependent loads. To understand the dynamics of the coupled flow-structure system, it is customary to study prototype flows around bluff bodies, whose motion is prescribed externally, characterized by the non-dimensional values of the oscillation amplitude and frequency.

A large volume of studies, including the experiments of Bishop and Hassan [1], Williamson and Roshko [2], Gopalkrishnan [3] and the numerical studies of Blackburn and Henderson [4], Anagnostopoulos [5], Kaiktsis et al. [6], has addressed the problem of flow past a cylinder forced to vibrate transversely to a free stream.

In contrast to the large body of literature studies on the flow past a cylinder oscillating transversely to the free stream, few studies have examined the more realistic case of the flow past a cylinder vibrating both transversely and in-line to the incoming flow. Experimental studies for a cylinder motion with two degrees of freedom include the one of Jeon and Gharib [7], who conducted experiments by forcing a cylinder to move both in the in-line and transverse directions. In their work, the frequency of the in-line motion is twice that of the transverse motion; thus the cylinder follows a trajectory resembling an "eight" figure. Their results indicate that, while the frequency of vortex shedding is still determined by the transverse motion, the streamwise motion controls the phase of shedding, and thus the phase of the instantaneous lift force, determining the energy transfer to the cylinder.

In the present study, we perform detailed numerical simulations of two-dimensional flow past a cylinder vibrating both transversely and in-line with respect to a uniform stream, extending our previous work of flow past a cylinder vibrating only in the transverse direction (Kaiktsis et al. [6]). For a flow from left to right, depending on the direction of the cylinder motion in the upper half plane, we distinguish between a "counter-clockwise" and a "clockwise" oscillation mode. Here, we consider transverse oscillation frequencies equal to or close to the Strouhal frequency. Two representative ratios of the in-line vibration amplitude to the transverse amplitude are considered, equal to 0.2 and 0.4, while the values of transverse-amplitude-over-diameter-ratio correspond to excitation, i.e. positive power transfer from the fluid to the cylinder. We calculate the non-dimensional values of the power transfer from the fluid to the body, and the forces acting on the cylinder, and correlate the results to the structure of the wake.

NOMENCLATURE

$\varepsilon = \frac{A_x}{A_y}$	amplitude ratio
η_x	instantaneous displacement of the cylinder in the x-direction
η_y	instantaneous displacement of the cylinder in the y-direction
v	fluid kinematic viscosity
ρ	fluid density
A_x	in-line oscillation amplitude
A_y	transverse oscillation amplitude
C_D	drag coefficient
C_L	lift coefficient
D	cylinder diameter
$F = \frac{f_y}{f_s}$	frequency ratio
F_y	lift force
F_x	drag force
f_s	Strouhal frequency
f_x	in-line vibration frequency
f_y	transverse vibration frequency
Re	Reynolds number
T	integration time
U_∞	free-stream velocity

PROBLEM DEFINITION AND NUMERICAL METHOD

In this study, we consider a cylinder vibrating both transversely and in-line to a uniform stream, following an "eight"–like trajectory. The cylinder has a diameter, D, the velocity of the fluid far upstream is U_∞, while the density and kinematic viscosity of the fluid are ρ and v, respectively. The coordinate axes are x, parallel to the incoming flow, and y, normal to the flow. The cylinder is oscillating around a mean position, with transverse amplitude A_y and frequency f_y, and in-line amplitude A_x and frequency f_x. The in-line vibration frequency is twice the transverse frequency, $f_x=2f_y$; thus the cylinder follows an "eight"–like trajectory. The instantaneous displacement of the cylinder in the y- and x-directions is:

$$\eta_y = A_y \sin(2\pi f_y t) \tag{1}$$

$$\eta_x = \pm A_x \sin(2\pi f_x t) = \pm A_x \sin(4\pi f_y t) \tag{2}$$

For a flow stream from left to right, the plus (+) sign in Eq. (2) corresponds to a motion which is counter-clockwise in the upper x-y plane, and the minus (-) sign to a clockwise motion in the upper x-y plane.

The total lift and drag force, per cylinder unit length, are scaled with the dynamic pressure, yielding the lift and drag coefficient, respectively:

$$F_y = \frac{1}{2}\rho U_\infty^2 D C_L \tag{3}$$

$$F_x = \frac{1}{2}\rho U_\infty^2 D C_D \tag{4}$$

From dimensional analysis it follows that all non-dimensional force coefficients are functions of the Reynolds number, of the normalized y-amplitude $\frac{A_y}{D}$, the amplitude ratio $\varepsilon = \frac{A_x}{A_y}$, and the frequency ratio $F = \frac{f_y}{f_s}$ (where f_s is the natural frequency of the Kármán vortex street). Each of the two directions in which the "eight" trajectory is traversed defines a different physical problem, thus the dynamics also depends on the oscillation mode ("counter-clockwise" or "clockwise").

The time-averaged power transferred from the flow to the cylinder (per cylinder unit length) can be normalized by $\frac{1}{2}\rho U_\infty^3 D$ to yield the non-dimensional "power transfer parameter". In the presence of both in-line and transverse cylinder oscillation, the total power transfer parameter, P, consists of the sum of the corresponding contributions:

$$P = \frac{2}{\rho U^3 D}\frac{1}{T}\{\int_o^T F_y \frac{d\eta_y}{dt}dt + \int_0^T F_x \frac{d\eta_x}{dt}dt\} \tag{5}$$

The power transfer parameter is an important quantity for vortex-induced vibrations, as positive values correspond to excitation, and negative values to damping.

We solve the Navier–Stokes equations for Newtonian incompressible flow. To avoid reconstructing the computational grid at each time step, we use coordinates that are fixed on the cylinder. We non-dimensionalize with respect to D and U_∞. Thus, the governing equations can be written as follows:

$$\nabla \cdot \vec{u} = 0 \tag{6}$$

$$\frac{\partial \vec{u}}{\partial t} + \vec{u}\cdot\nabla\vec{u} = -\nabla p + \frac{1}{\mathrm{Re}}\nabla^2\vec{u} - \frac{d^2\eta_x}{dt^2}\vec{i} - \frac{d^2\eta_y}{dt^2}\vec{j} \tag{7}$$

where $\vec{u}$ is the fluid velocity with respect to the moving cylinder, p is the pressure, and $\mathrm{Re} = U_\infty D / \nu$ is the Reynolds number of the flow. Throughout the paper, the Reynolds number is equal to 400, a value identical to the one of Kaiktsis et al. [6], and close to that in the experiments of Williamson and Roshko [2].

In order to find the actual force components acting on the cylinder, we subtract from the computed lift and drag forces a "dynamic Archimedes" force, equal to $-(\frac{\pi}{4})\rho D^2 d^2\eta_y / dt^2\vec{j}$ and $-(\frac{\pi}{4})\rho D^2 d^2\eta_x / dt^2\vec{i}$, for the lift and drag force, respectively.

The velocity boundary conditions for the flow are implemented as follows: (i) at the inflow and lateral boundaries, $\vec{u}_x = (1 - \frac{d\eta_x}{dt})\vec{i}$, $\vec{u}_y = -\frac{d\eta_y}{dt}\vec{j}$, (ii) on the cylinder $\vec{u} = 0$, (iii) at the outflow boundary we assume a Neumann condition, $\partial\vec{u}/\partial\eta = 0$.

Eqs. (6), (7) subject to the above boundary conditions are solved using a Legendre spectral element method, e.g. see Karniadakis and Sherwin [8], with the time discretization based on a second-order accurate mixed stiffly stable scheme (Karniadakis et al., [9]). The spectral element skeleton used, which is identical to that in Kaiktsis et al. [6], is shown in Fig. 1. The inflow boundary is located at *x/D=-20*, the lateral boundaries at *y/D=±17*, and the outflow boundary at *x/D=60*. The spatial discretization consists of 464 macro-elements, with 9x9 elemental resolution. Typically, the values of the non-dimensional numerical time step were in the range 0.00075 to 0.0015.

RESULTS

In this section, we present computational results for three values of frequency ratio, $F=f_y/f_s$, equal to 0.9, 1.0 and 1.1, corresponding to below-resonant, resonant and above-resonant forcing frequencies. Two values of amplitude ratio $\varepsilon=A_x/A_y$ are considered, equal to 0.2 and 0.4, for both the counter-clockwise and clockwise modes. The governing equations are integrated until a "statistical steady state" is reached, within which the flow mean quantities are time-independent. The reported flow statistics correspond to this state. In general, computations are performed up to amplitudes for which negative values of the power transfer parameter are obtained.

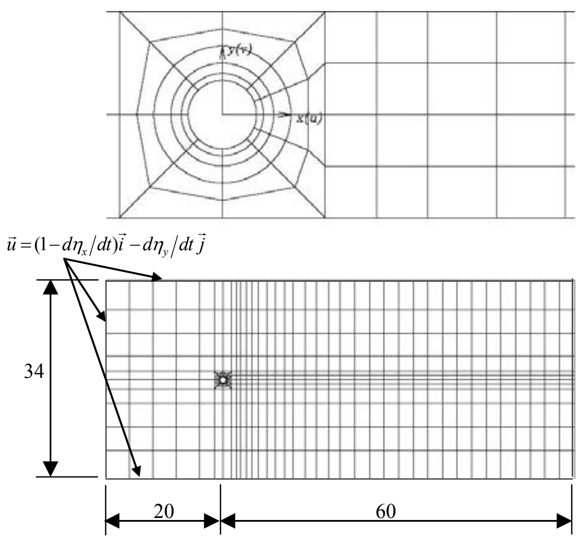

Fig. 1. Spectral element skeleton for flow past a circular cylinder, including elements close to the cylinder, and the entire mesh. Velocity boundary conditions for a coordinate system fixed on the cylinder are also indicated.

Power transfer and hydrodynamic forces

The variation of the power transfer parameter P with the transverse oscillation amplitude is shown in Figs 2 and 3, for F = 0.9 (ε = 0.2 and 0.4). Figs 2 and 3 demonstrate that, both for ε = 0.2 and ε = 0.4, the "counter-clockwise" motion is associated with an increased amplitude range of positive P values, in comparison to the other two oscillation modes (transverse-only oscillation and clockwise motion). The corresponding variation of time-averaged drag coefficient for ε = 0.2 is presented in Fig. 4. The drag force is an increasing function of oscillation amplitude, with higher levels corresponding to the counter-clockwise oscillation mode.

For F = 1, the variation of power transfer parameter with oscillation amplitude is shown in Fig. 5, and the corresponding variation of drag coefficient in Fig. 6 (ε = 0.2). In the counter-clockwise motion, the range of A_y/D corresponding to positive P is larger, in comparison to the other two oscillation modes. In addition, Fig. 6 demonstrates that, in comparison to transverse-only oscillation, the presence of in-line motion increases, in most cases, the drag forces exerted on the cylinder.

Finally, we consider the case where the cylinder is forced to oscillate with an excitation frequency equal to 1.1 times the natural frequency of vortex shedding (F = 1.1). The variation of the power transfer parameter and drag coefficient with oscillation amplitude, for ε = 0.2, is shown in Figs 7 and 8, respectively. The variation of P is characterized by alterations between positive and negative values, with the maximum values of positive P being lower in comparison to the cases of resonant and below-resonant forcing. With respect to the drag force, the variations are also non-monotonic and quite complex.

The flow dynamics can be characterized by considering the spectra of the computed lift coefficient signals. Figs 9 and 10 present the spectra corresponding to counter-clockwise motion at F = 0.9, for transverse oscillation amplitudes equal to *0.1D* and *0.4D*, respectively. Figs 11 and 12 present the corresponding spectra for clockwise motion. In all cases, the flow is locked-in to the excitation frequency, even at the low amplitude. For the counter-clockwise mode, the frequency content becomes rich at high amplitude, while a strong peak at the third harmonic is present at both amplitudes. For the clockwise mode, odd harmonics are present in the spectrum at low amplitude, and both odd and even harmonics at high amplitude. The presence of the third harmonic remains pronounced at F = 1.0 (Figs 13 and 14), while the spectra are characterized by very rich frequency content for F = 1.1 (Figs 15 and 16).

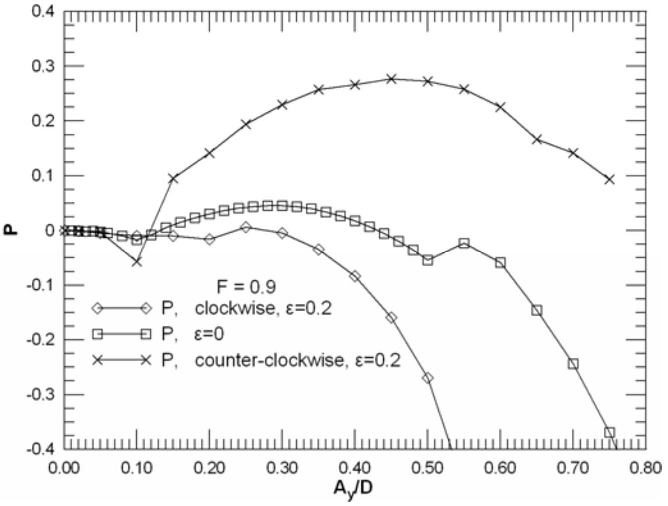

Fig. 2. Non-dimensional total power transfer, *P*, versus the reduced y-amplitude, for frequency ratio $F = f_y/f_s = 0.9$; here, the cases $\varepsilon = 0$ (transverse-oscillation only), and $\varepsilon = 0.2$ (counter-clockwise and clockwise modes) are considered.

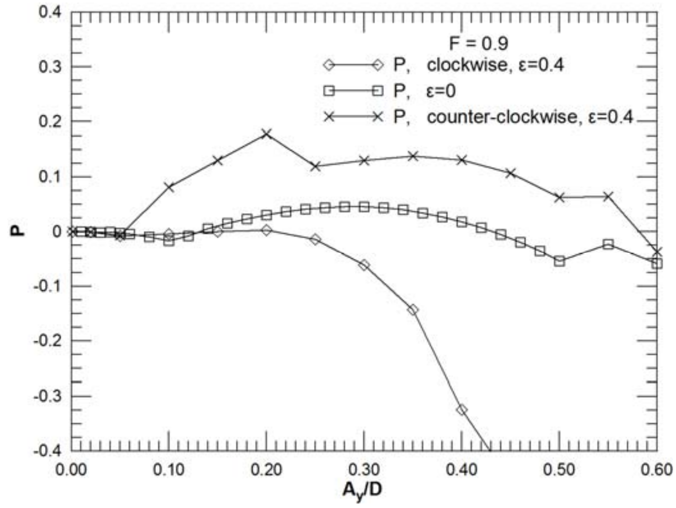

Fig. 3. Non-dimensional total power transfer, *P*, versus the reduced y-amplitude, for frequency ratio $F = f_y/f_s = 0.9$; here, the cases $\varepsilon = 0$ (transverse-oscillation only), and $\varepsilon = 0.4$ (counter-clockwise and clockwise modes) are considered.

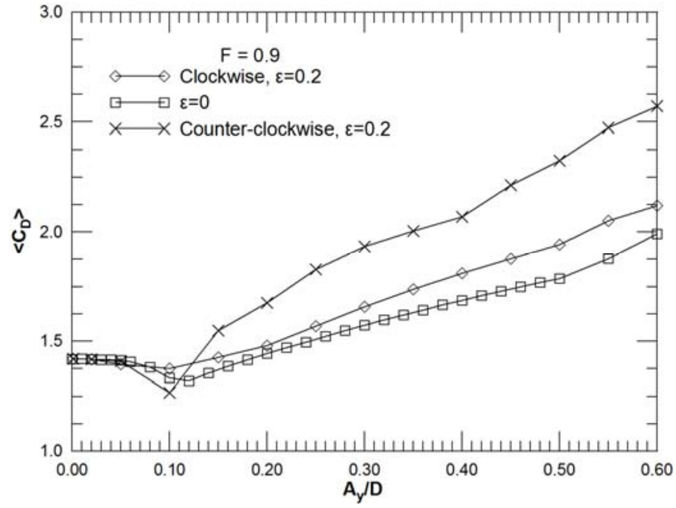

Fig. 4. Time-averaged drag coefficient versus the reduced y-amplitude, for frequency ratio $F = f_y/f_s = 0.9$; here, the cases $\varepsilon = 0$ (transverse-oscillation only), and $\varepsilon = 0.2$ (counter-clockwise and clockwise modes) are considered.

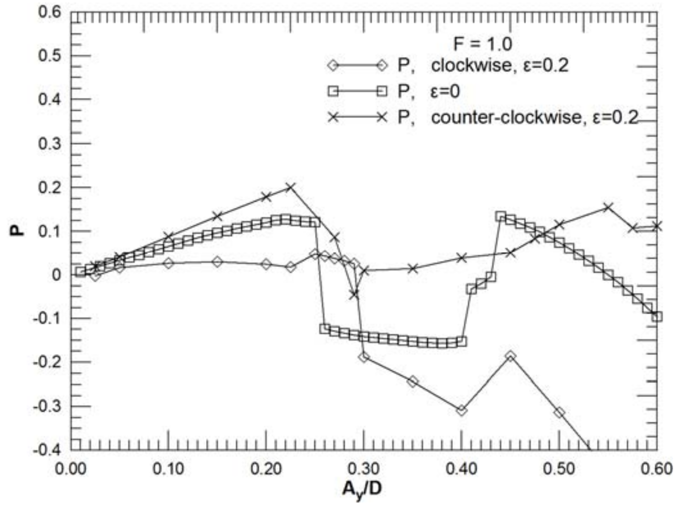

Fig. 5. Non-dimensional total power transfer, *P*, versus the reduced y-amplitude, for frequency ratio $F = f_y/f_s = 1.0$; here, the cases $\varepsilon = 0$ (transverse-oscillation only), and $\varepsilon = 0.2$ (counter-clockwise and clockwise modes) are considered.

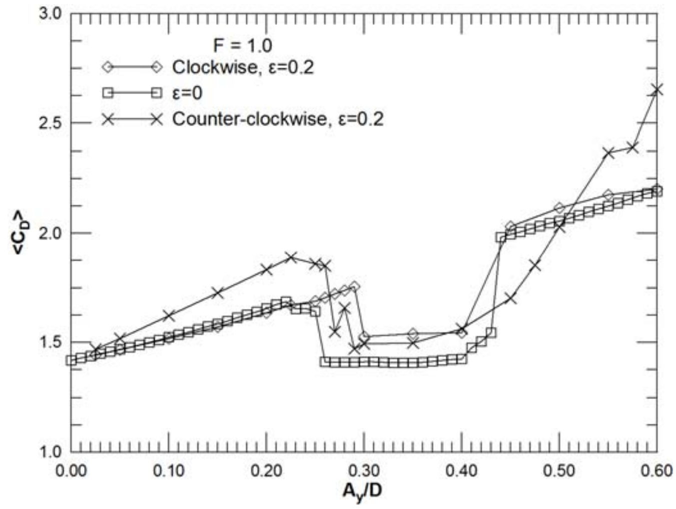

Fig. 6. Time-averaged drag coefficient versus the reduced y-amplitude, for frequency ratio $F = f_y/f_s = 1.0$; here, the cases $\varepsilon = 0$ (transverse-oscillation only), and $\varepsilon = 0.2$ (counter-clockwise and clockwise modes) are considered.

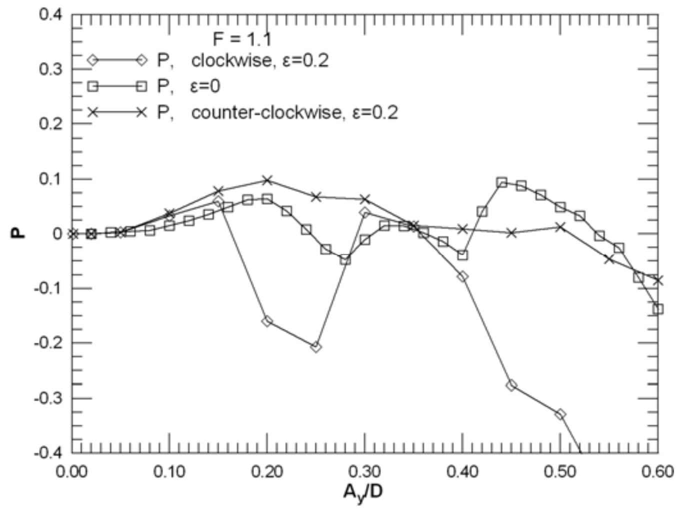

Fig. 7. Non-dimensional total power transfer, P, versus the reduced y-amplitude, for frequency ratio $F = f_y/f_s = 1.1$; here, the cases $\varepsilon = 0$ (transverse-oscillation only), and $\varepsilon = 0.2$ (counter-clockwise and clockwise modes) are considered.

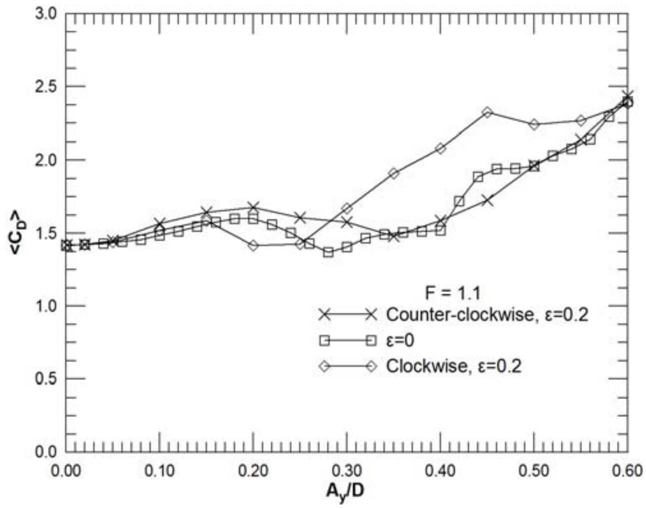

Fig. 8. Time-averaged drag coefficient versus the reduced y-amplitude, for frequency ratio $F = f_y/f_s = 1.1$; here, the cases $\varepsilon = 0$ (transverse-oscillation only), and $\varepsilon = 0.2$ (counter-clockwise and clockwise modes) are considered.

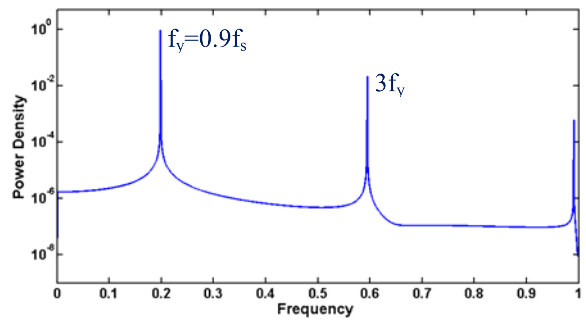

Fig. 9. Lift coefficient spectrum for a case with frequency ratio $F = f_y/f_s = 0.9$, counter-clockwise cylinder motion, $\varepsilon = 0.2$, and transverse oscillation amplitude $A_y/D = 0.10$.

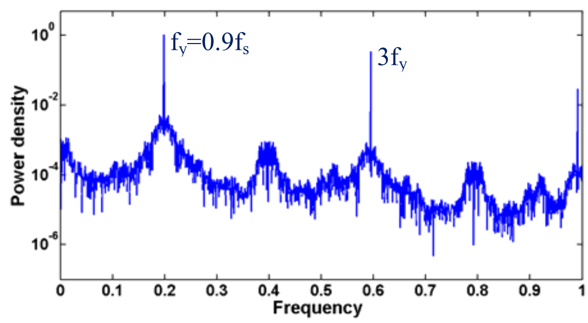

Fig. 10. Lift coefficient spectrum for a case with frequency ratio $F = f_y/f_s = 0.9$, counter-clockwise cylinder motion, $\varepsilon = 0.2$, and transverse oscillation amplitude $A_y/D = 0.40$.

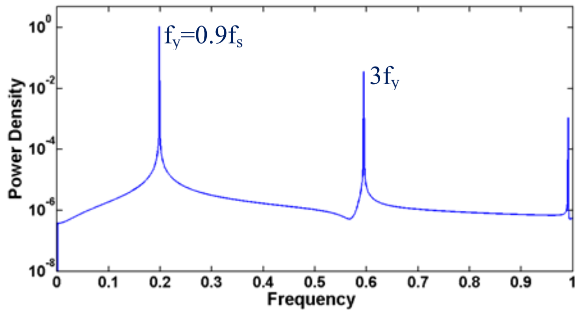

Fig. 11. Lift coefficient spectrum for a case with frequency ratio *F = f_y/f_s = 0.9*, clockwise cylinder motion, *ε = 0.2*, and transverse oscillation amplitude *A_y/D = 0.10*.

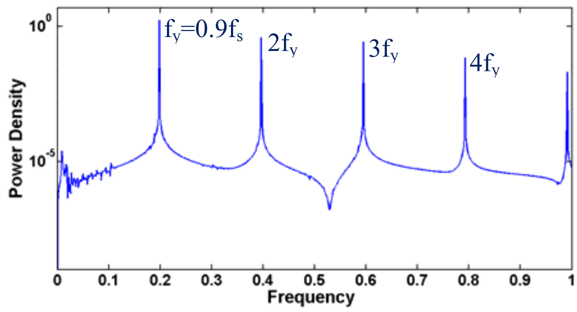

Fig. 12. Lift coefficient spectrum for a case with frequency ratio *F= f_y/f_s = 0.9*, clockwise cylinder motion, *ε = 0.2*, and transverse oscillation amplitude *A_y/D = 0.40*.

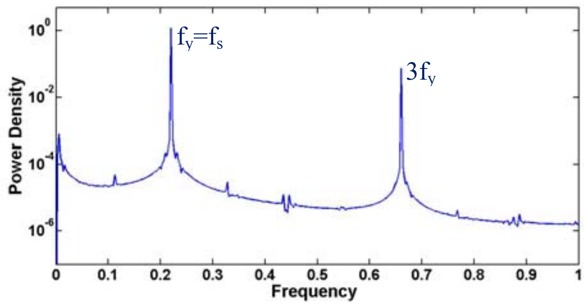

Fig. 13. Lift coefficient spectrum for a case with frequency ratio *F = f_y/f_s = 1.0*, counter-clockwise cylinder motion, *ε = 0.2*, and transverse oscillation amplitude *A_y/D = 0.10*.

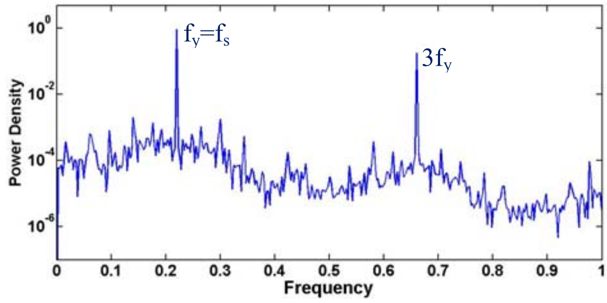

Fig. 14. Lift coefficient spectrum for a case with frequency ratio *F = f_y/f_s = 1.0*, counter-clockwise cylinder motion, *ε = 0.2*, and transverse oscillation amplitude *A_y/D = 0.40*.

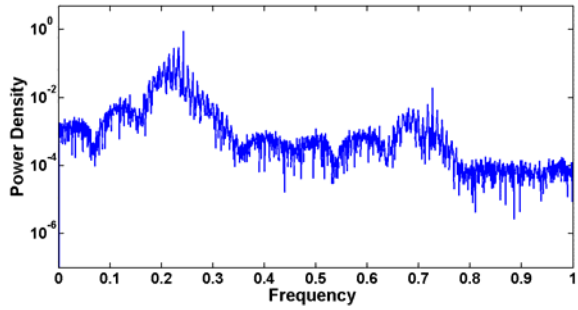

Fig. 15. Lift coefficient spectrum for a case with frequency ratio *F = f_y/f_s = 1.1*, counter-clockwise cylinder motion, *ε = 0.2*, and transverse oscillation amplitude *A_y/D = 0.10*.

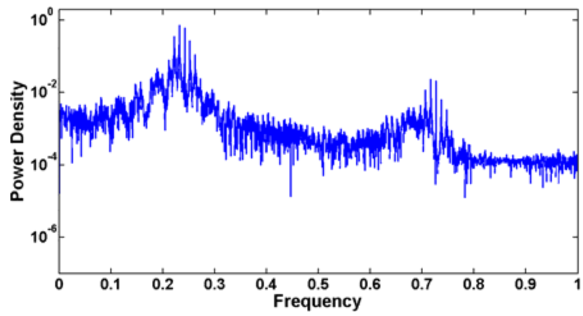

Fig. 16. Lift coefficient spectrum for a case with frequency ratio *F = f_y/f_s = 1.1*, clockwise cylinder motion, *ε = 0.2*, and transverse oscillation amplitude *A_y/D = 0.10*.

Visualization of the flow in the wake

In this section, we present visualizations of the wake in terms of vorticity isocontours. The visualizations correspond to the moment that the cylinder occupies its mean position (η_y/D= η_x/D=0). The flow visualizations illustrate the structure of the vortex street, and can be related to the variations of the forces on the cylinder, although the relation is by no means straightforward. For brevity, visualizations are only presented for ε = 0.2 and counter-clockwise oscillation mode.

Representative flow visualizations for the three oscillation frequencies of the present study are shown in Figs 17, 18 and 19. For frequency ratios less than or equal to 1.0, the vortex street is characterized by a 2S type mode, at low amplitudes. As the amplitude increases, the state of the wake becomes disordered, with complex vortex patterns. For higher frequency ratio (F = 1.1), 2S structures are present in the near wake at low oscillation amplitude, becoming more complicated downstream. At higher amplitudes, the vortex patterns in the wake remain complex, dominated by triplets or other combinations of vortices.

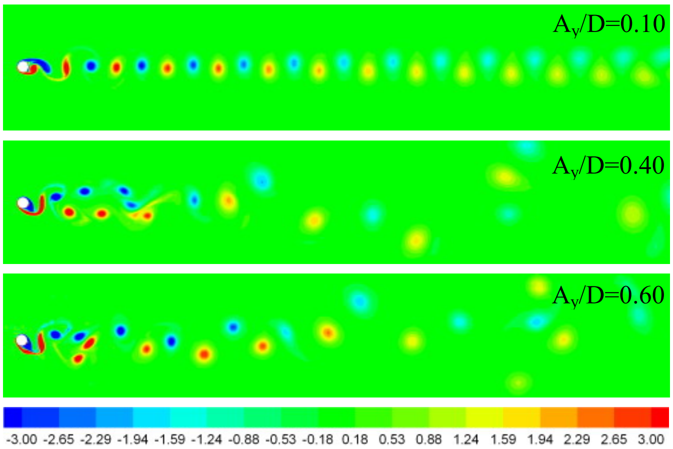

Fig. 17. Instantaneous vorticity isocontours for frequency ratio *$F = f_y/f_s$ = 0.9,* counter-clockwise cylinder motion, *ε = 0.2,* and transverse oscillation amplitudes *A_y/D = 0.10, 0.40, 0.60.*

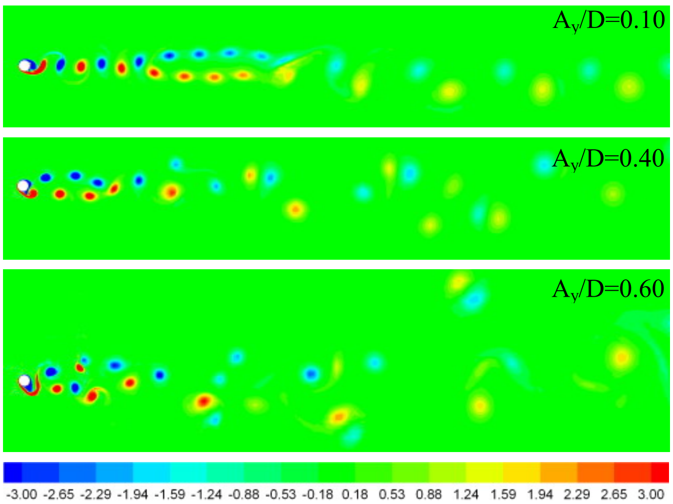

Fig. 18. Instantaneous vorticity isocontours for frequency ratio *$F = f_y/f_s$ = 1.0,* counter-clockwise cylinder motion, *ε = 0.2,* and transverse oscillation amplitudes *A_y/D = 0.10, 0.40, 60.*

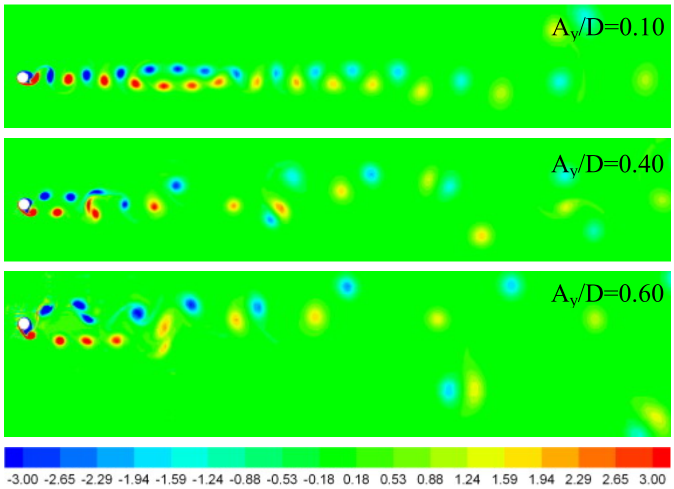

Fig. 19. Instantaneous vorticity isocontours for frequency ratio *$F = f_y/f_s$ = 1.1,* counter-clockwise cylinder motion, *ε = 0.2,* and transverse oscillation amplitudes *A_y/D = 0.10, 0.40, 60.*

CONCLUSIONS

In this paper, we have presented computational results of the flow structure and forces on a cylinder oscillating both transversely and in-line to a steady stream, at Reynolds number *Re=400*. Here, the cylinder follows an "eight"-like trajectory, as in free vortex-induced vibration. For a flow stream from left to right, we have studied both the "counter-clockwise" and "clockwise" oscillation modes (corresponding to a counter-clockwise or clockwise cylinder motion in the upper part of the trajectory, respectively). Two values of the in-line to the transverse oscillation amplitude were considered, ε=0.2 and ε=0.4, and the results were compared against the ε=0 case (transverse-only oscillation). The oscillation amplitude was varied from zero to values corresponding to negative power transfer from the flow to the cylinder. Three values of transverse oscillation frequency were considered, corresponding to F= 0.9, 1.0 and 1.1.

The present study has demonstrated that the “counter-clockwise” mode is in general associated with higher non-dimensional forces than the “clockwise” mode. For the “counter-clockwise” motion, the power transfer to the cylinder remains, in general, positive for higher oscillation amplitudes, in comparison to the “clockwise” motion; for ε=0.2, these oscillation amplitude values are also higher in comparison to those of the case of transverse-only oscillation. Thus, the “counter-clockwise” motion appears to be the most dangerous one for applications of vortex-induced vibrations. We believe that both modes may be present in vortex-induced vibrations, with the system selection of the mode depending on the details of the set-up and initial conditions.

In general, the observed wakes are characterized by 2S structure at low amplitudes, and more complicated wake structure at high amplitudes, especially at higher values of amplitude ratio ε, i.e. at higher in-line oscillation amplitudes.

This tendency towards complex and chaotic flow states at increasing in-line oscillation amplitude should be interpreted on the basis of the pattern competition between two modes, a symmetric flow mode due to the in-line oscillation and the asymmetric mode of the Kármán street, with entirely different spatial structures, see Ciliberto and Gollub [10], Perdikaris et al. [11].

Overall, the following two important effects of the presence of in-line oscillation on the hydrodynamic forces acting on the cylinder should be underlined: (1) the existence of a strong third harmonic component in the spectrum of the lift force, for transverse oscillation frequencies less than or equal to the Strouhal frequency. This can cause higher fatigue stresses on vibrating structures. (2) The aperiodic character of lift forces in the counter-clockwise mode, for frequency ratios less than or equal to 1 and moderate to high oscillation amplitudes, as well as the complexity of force signals, for both the counter-clockwise and the clockwise mode, at higher frequency ratios.

REFERENCES

[1] Bishop, R. E. D., and Hassan, A. Y., 1964, "The Lift and Drag Forces on a Circular Cylinder Oscillating in a Flowing Fluid", Proceedings of the Royal Society, Series A, 277, pp. 51-75.

[2] Williamson, C. H. K., and Roshko, A., 1988, "Vortex Formation in the Wake of an Oscillating Cylinder", Journal of Fluids and Structures, 2, pp. 355-381.

[3] Gopalkrishnan, R., 1993, "Vortex-Induced Forces on Oscillating Bluff Cylinders", Ph.D. Thesis, MIT, Cambridge, MA.

[4] Blackburn, H. M., and Henderson, R. D., 1999, "A Study of Two-Dimensional Flow Past an Oscillating Cylinder", Journal of Fluid Mechanics, 385, pp. 255-286.

[5] Anagnostopoulos, P., 2000, "Numerical Study of the Flow Past a Cylinder Excited Transversely to the Incident Stream. Part 1: Lock-in Zone, Hydrodynamic Forces and Wake Geometry", Journal of Fluids and Structures, 14(6), pp. 819-851.

[6] Kaiktsis, L., Triantafyllou, G. S., and Ozbas, M., 2007, "Excitation, Inertia, and Drag Forces on a Cylinder Vibrating Transversely to a Steady Flow", Journal of Fluids and Structures, 23(1), pp. 1-21.

[7] Jeon, D., and Gharib, M., 2001, "On Circular Cylinders Undergoing Two-Degree-Of-Freedom Forced Motions", Journal of Fluids and Structures, 15, pp. 533–541.

[8] Karniadakis, G. E., and Sherwin, S.J., 1999, "Spectral/hp Element Methods for CFD", Oxford University Press.

[9] Karniadakis, G. E., Israeli, M., and Orszag, S. A., 1991, "High-Order Splitting Methods for the Incompressible Navier–Stokes Equations", Journal of Computational Physics, 97, pp. 414–443.

[10] Ciliberto S., and Gollub J. P., 1984, "Pattern Competition Leads to Chaos", Physical Review Letters, 52, pp. 922-925.

[11] Perdikaris, P. G., Kaiktsis, L., and Triantafyllou, G. S., 2009, "Chaos in a Cylinder Wake due to Forcing at the Strouhal Frequency", Physics of Fluids, 21, Paper No101705, pp. 1-3.